Discriminating Familiarity In Face Perception Through Eeg And Erp Analysis With Confident Learning Techniques

M. Subathra
Assistant Professor, Department of Computer Applications,
Vellalar College for Women (Autonomous), Erode.
subathra@vcw.ac.in

Abstract

Despite the time-consuming nature of data gathering, EEG is an essential tool for researching human perception. FUFP, the largest publicly available EEG dataset for familiar versus unfamiliar face perception, is presented in this paper. It includes 6,400 samples from 8 participants across 66 channels. Five basic machine learning models demonstrate that familiarity categorization is feasible. Event-related potential (ERP) research supports this claim by showing higher N400 components for unfamiliar faces. A deep learning strategy is proposed to enhance feature emphasis and data quality by combining ERP insights with confident learning (ECL). This approach outperforms current models, and FUFP is recommended for further research.

Keywords: EEG; face perception; familiarity classification; neurobiological signal processing.

1. Introduction

Face perception is a key area of research due to its fundamental role in enabling humans to interact and communicate effectively within society. Since faces convey a wide range of social cues, many studies have used face perception as a framework to investigate the structure and function of the human brain. Unlike other visual stimuli, faces hold a special status because of their strong biological, personal, and social relevance. This significance is evident in how quickly and efficiently the human visual system can detect faces, often prioritizing them over other visual inputs. The brain can initiate extremely fast eye movements—known as saccades—toward faces in as little as 100 milliseconds, by leveraging distinct low-level facial features.

Most people can easily recognize familiar individuals by interpreting facial features, but this ability is not universal. Some individuals experience prosopagnosia, a neurological condition characterized by difficulty in recognizing familiar faces—including their own—typically due to damage in the brain's fusiform face area (FFA). Research by DeGutis et al. revealed that the prevalence of prosopagnosia is higher than previously estimated, affecting approximately 3.08% of the population, or about 1 in every 33 people.

Traditionally, prosopagnosia is diagnosed using self-reported questionnaires or structured interviews. However, the diagnostic standards vary widely between studies, and the subjective nature of these methods can impact accuracy. Factors such as social stigma, embarrassment, or miscommunication can prevent individuals from providing honest or accurate responses. As a result, there is a growing shift toward objective, computer-based face recognition assessments, which offer more consistent and reliable tools for identifying this condition.

EEG, as a type of biomedical signal, has significant applications across various domains, including epilepsy detection, preference analysis, sleep disorder diagnosis, identity verification, and visual perception.By recording EEG signals from participants as they view faces with varying degrees of familiarity, and applying machine learning algorithms to extract and classify the features, researchers can objectively assess conditions like prosopagnosia.

Beyond its utility in diagnosing prosopagnosia, EEG-based familiarity classification—determining whether the subject saw a familiar or unfamiliar face—can also support early detection of mild cognitive impairment (MCI). Additionally, analyzing EEG responses to faces with different levels of familiarity contributes to our understanding of the neural mechanisms behind face perception, further advancing cognitive neuroscience.

2. Related Works

Machine learning plays a central role in EEG research. For instance, Tasci et al. developed a feature extraction technique inspired by black–white hole patterns from astrophysics to identify chronic neuropathic pain. In another study, they introduced a hypercube-based feature extractor that combines various statistical properties and neighborhood component analysis to enhance epilepsy detection. Lan et al. proposed a feature selection strategy aimed at identifying stable emotional features, thereby addressing the long-term performance degradation in affective brain–computer interfaces (aBCIs). Meanwhile, Li et al. presented three data augmentation methods for EEG analysis that do not rely on parameter learning.

Deep learning has increasingly outperformed traditional machine learning approaches in EEG analysis due to its ability to automatically extract complex features and model non-linear patterns. Several researchers have leveraged deep neural networks to advance EEG signal processing. For instance, Lan et al. applied transductive transfer learning to transfer knowledge between datasets, improving classification accuracy across different data domains. Kumari et al. integrated War Strategy Optimization (WSO) and the Chimp Optimization Algorithm (CHOA) to enhance deep learning models, specifically using a CNN and a modified DNN for motion imagery channel classification.

Li et al. developed a subject-matching framework leveraging multi-source domain adaptation to assess situation awareness across individuals in latent EEG space. In a separate study, they introduced a batch normalization time-frequency transformer designed to extract global EEG features for detecting driver fatigue. Tuncer et al. integrated classical and deep learning methodologies, combining nonlinear features—such as statistical moments and textures—and employing feature selection techniques like RelieF to enhance emotional state recognition from EEG signals.

In the realm of familiar versus unfamiliar face classification using EEG, both traditional and deep learning approaches have been explored. Ozbeyaz et al. utilized distance- and similarity-based algorithms to pinpoint key channels and time windows for effective classification. Ghosh et al. developed a deep learning model capable of capturing both temporal and spatial features, yielding strong results in distinguishing familiar from unfamiliar faces. Meanwhile, Williams et al. implemented a sparse ensemble classifier to examine ERP signals as potential biomarkers for diagnosing mild cognitive impairment.

Bablani et al. created a concealed information test based on EEG responses to familiar and unfamiliar faces. Chang et al. used classifiers like SVM and KNN to develop a face recognition system using directed functional brain networks. William et al. combined convolutional neural networks (CNNs) with random forests to classify face familiarity from a very limited dataset. Wiese et al. applied logistic regression to ERP data to determine face familiarity.

Despite the progress in EEG-based face familiarity classification, much of the existing research has been conducted on private datasets, limiting reproducibility and comparative analysis across studies. Currently, there is no standardized, publicly available benchmark dataset specifically focused on this task. This gap presents a challenge for consistent evaluation and development of advanced algorithms. A publicly accessible dataset would serve as a valuable resource for the research community, enabling fair comparison between methods and fostering further innovation in the field of EEG-based face perception analysis.

While much of the prior research has concentrated on traditional machine learning and deep learning methods for EEG analysis, less attention has been given to classical EEG analysis techniques such as Event-Related Potential (ERP) analysis. ERP is particularly valuable for studying face familiarity, as it captures time-locked neural responses linked to specific cognitive events. In this work, we integrate insights from ERP analysis with deep learning, utilizing attention mechanisms to emphasize key temporal features related to facial recognition.

One of the key challenges in EEG-based classification is the presence of artifacts during signal acquisition and potential labeling errors arising from repeated trials. These issues can significantly affect model performance. To address this, we introduce a deep learning framework based on **ERP-guided Confident Learning (ECL)**. This approach not only helps in filtering noisy data but also enhances model accuracy by refining the training process through more reliable feature extraction and error correction.

Main Contributions

1. FUFP Dataset Compilation: We developed and published the FUFP dataset, now the most extensive publicly accessible EEG dataset for face familiarity research. It facilitates rapid advancement and comparison of signal processing and classification techniques. The dataset comprises six labeling categories, enabling more detailed assessments—including an identifier specifying whether the face belongs to the subject themselves.

2. Benchmark Establishment: We present benchmark findings utilizing five baseline classifiers, accompanied by ERP and power spectral density (PSD) evaluations, to aid and direct upcoming research in EEG-based face familiarity studies.

3. ECL Algorithm Introduction: We introduce a novel approach, ECL (ERP analysis and Confident Learning), for distinguishing responses to familiar and unfamiliar face stimuli. Experimental analyses conducted on the FUFP dataset affirm the effectiveness of this methodology.

This paper is structured as follows: Section 2 elaborates on the design and acquisition process of the FUFP dataset. Section 3 outlines benchmark experiment outcomes obtained using the dataset to assess baseline performance. In Section 4, we describe the proposed ECL algorithm, present experimental results, and examine the model's complexity. Section 5 discusses the dataset, methodology, benefits, and limitations of our approach. Finally, Section 6 wraps up the paper, summarizing major contributions and suggesting potential directions for future research.

3. METHODOLOGY

3.1. Participants

Eight volunteers took part in the experiment, consisting of four males and four females, all between the ages of 22 and 25, with an average age of 23.6 years. All participants had normal or corrected-to-normal vision and no physical impairments. They were all members of the same laboratory and were acquainted with one another. To comply with privacy regulations, participants' identities were anonymized and referred to as "Subject 1" through "Subject 8."

3.2. Stimulus Materials

In accordance with the oddball paradigm [4], the stimulus set included 20% frequently familiar (FF) faces and 80% unfamiliar (UF) faces. The FF stimuli were derived from student ID photographs of the eight participants, all of whom were familiar with one another. The UF stimuli comprised 32 frontal facial images of young individuals, selected from the CAS-PEAL-R1 dataset [35]. Altogether, 40 facial images were utilized. Each image was edited to remove background elements and irrelevant details, converted to grayscale, and resized to a consistent dimension of 360 × 480 pixels.

3.3. Experimental Paradigm

EEG data were collected using the Neuroscan Synamps2 amplifier at a sampling rate of 1000 Hz, with data analysis performed using Curry8 software. Neuroscan Synamps2 is used for recording brain signals, while Curry8 helps with data processing tasks such as filtering, artifact removal, baseline correction, and time–frequency analysis. A total of 64 electrodes were placed on each participant's scalp based on the standard 10–20 system (see Figure 1), with additional electrodes for recording eye movements (VEO and HEO) shown in Figure 2.

Before the experiment, participants cleaned their scalps and applied conductive paste to ensure good contact between the electrodes and skin, reducing signal resistance. The experiment took place in a quiet, electrically shielded room to minimize distractions. The facial images were shown at the center of the screen, and participants sat at a fixed distance from it. A keyboard was provided for responses, and participants could stop the experiment at any time.

The experiment had two main parts: a practice session and the actual test. First, a message saying "the experiment is about to start" appeared for 10 seconds. During the practice phase, a white cross appeared for 2 seconds to help participants focus, followed by a number (1 or 2) displayed for 2 seconds. Participants pressed a button when the screen went black. After responding, feedback was given on accuracy and reaction time. This task was repeated five times to help participants get used to the setup.

In the main test, there were five blocks. Each block contained 40 trials, made up of 8 familiar and 32 unfamiliar face images presented in random order. Each trial followed the same sequence: a white cross appeared for 2 seconds to help the participant focus, followed by a face image displayed for 2 seconds. During this time, EEG signals were recorded as participants viewed and recognized the face. After the image, the screen turned black, and participants pressed "1" if they recognized the face or "2" if they didn't. After the response, the black screen remained for an additional 500 milliseconds to give a short break before the next image. This cycle continued until all 40 trials in the block were complet ed.

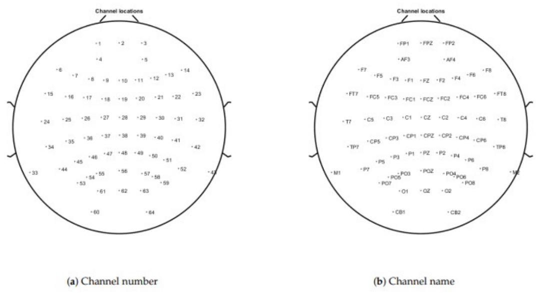

Figure 1: 2D Layout of 64 EEG Electrodes

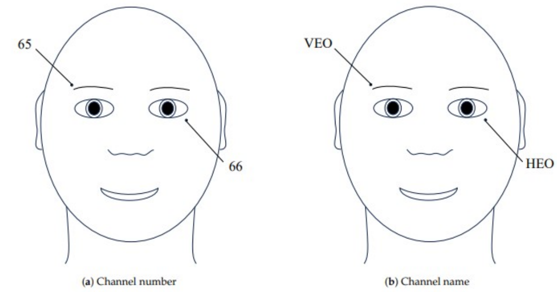

Figure 2:2D Location of two EOG electrodes, VEO and HEO.

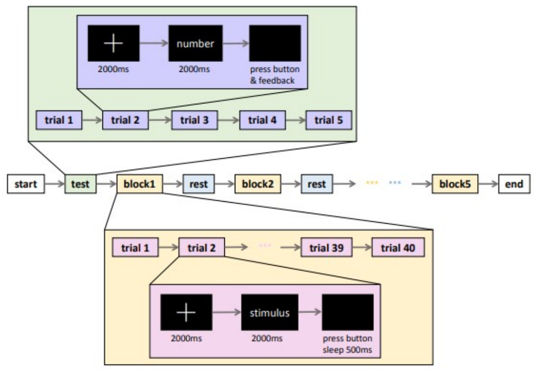

Figure 3: The whole experimental process.

The experiment was conducted four times for each participant to ensure accuracy and reliability. Instructions and short breaks were provided between different stages and blocks to avoid fatigue. Each session lasted around 20 minutes, resulting in a total experimental time of approximately 80 minutes per subject. Overall, the experiment included (8 familiar + 32 unfamiliar) trials × 5 blocks × 4 repetitions × 8 participants, resulting in a total of 6400 data samples.

3.4. Data Preprocessing

The EEG data recorded using Curry8 were automatically saved in CDT file format. To prepare the data for analysis and ensure accuracy, several preprocessing steps were applied:

1. Electrode Adjustment: Electrode positions from different subjects and sessions were aligned to a standard layout using Curry8. This step helps minimize differences between recordings and improves data consistency.
2. Baseline Correction: This correction was applied to eliminate slow signal drifts caused by the DC acquisition mode.
3. Bandpass Filtering: A bandpass filter was applied to keep only frequencies between 0 and 30 Hz, removing unwanted noise outside this range.
4. Removal of Eye Movement Artifacts: Signals from eye movements, like blinking, can distort EEG data. To remove these, Independent Component Analysis (ICA) was used to identify and eliminate components related to vertical eye movement activity.

3.5 ERP-Guided Neural Network Framework

ERP analysis from the previous section revealed that EEG signals vary in their ability to distinguish familiar and unfamiliar faces over time. Around 500 milliseconds, the N400 component was identified as a key marker for recognizing face familiarity. To make use of this information, we integrated ERP insights into a bidirectional long short-term memory (Bi-LSTM) neural network—originally introduced by Hochreiter et al. [8]—by incorporating attention weights based on ERP features.

Since EEG data often contain noise and labeling errors, which can affect the performance of neural networks that typically rely on large, clean datasets, we adopted confident learning [49] during training. This method uses cross-validation on the training set to identify and filter potentially mislabeled samples, reducing the negative impact of noisy data.

An overview of the proposed ERP-guided Confident Learning (ECL) algorithm is presented in Figure 1. The network architecture, including the input and output dimensions as well as the activation functions for each layer, is summarized in Table 1.

- The ERP-attention layer takes an input of 3000 features, corresponding to the length of the EEG signal, and reduces it to 198 features. This dimensionality reduction helps retain important temporal ERP characteristics.
- The initial Bi-LSTM layer takes in a 198-dimensional input from the ERP-attention layer and generates 128 feature representations.
- The second Bi-LSTM layer further compresses this to 64 features, extracting higher-level temporal patterns.
- A dense layer with an input and output of 64 units allows the model to learn deeper, more discriminative features.
- A final dense layer maps the 64 input features to 2 output categories, representing the two classification labels.

The training process involved three main stages:

1. **ERP Analysis:** EEG data were first examined to identify relevant temporal components.
2. **Pre-training with EBLM:** The ERP-based Bi-LSTM model underwent training, with cross-validation applied to evaluate the accuracy of label assignments.
3. **Confident Learning Application:** Using the predicted labels, confident learning estimated joint probabilities to detect mislabelled data. These samples were then

removed, and the model was retrained using the cleaned dataset.

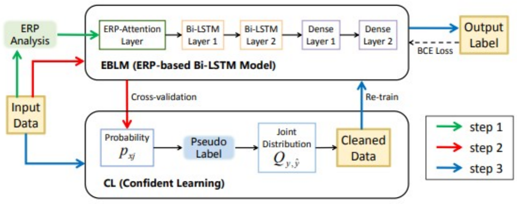

Figure 4: Architecture of ECL algorithm.

4.PROPOSED METHODOLOGY

4.1.1. EBLM (ERP-Based Bi-LSTM Model)

As illustrated in Figure 3, the EBLM module is composed of five main components: an ERP-attention layer, two bidirectional LSTM layers, and two dense layers.

The ERP-attention layer integrates the ERP analysis results into the model by assigning attention weights. These weights are computed using Equation (5).

$$\mathrm{Atten}(t) = \left| \frac{\sum_{i=1}^{M} FF_i(t)}{M} - \frac{\sum_{j=1}^{N} UF_j(t)}{N} \right|, \quad t \in (-500, 2500] \tag{1}$$

In the equation, tt signifies the time point of the EEG signal following ERP processing, while FF(t)FF(t) represents the amplitude of the EEG signal corresponding to the familiar face (FF) sample at time tt, and **UF(t)** refers to the amplitude of the EEG signal for the unfamiliar face (UF) sample at time **t**. **M** and **N** represent the total number of FF and UF samples, respectively. Figure 5 presents the calculated attention weights, illustrating the amplitude differences between FF and UF samples at each time point., which highlight the difference in amplitude between FF and UF samples at each time point. It is evident that the EEG signals around 500 ms are the most distinctive. To ensure proper scaling, the attention weights were normalized using Equation (2), so that their total sum equals 1.

$$Normal(t) = \frac{Atten(t)}{\sum_{i=-499}^{2500} Atten(i)} \tag{2}$$

The ERP-attention layer multiplies the input signals by the normalized attention weights, allowing the model to focus on the most relevant features. These weighted features are then passed into two identical Bi-directional Long Short-Term Memory (Bi-LSTM) layers. Bi-LSTM, a variant of recurrent neural network, analyzes time-series data bidirectionally—both forward and backward—allowing the model to capture richer temporal patterns.

After the Bi-LSTM layers, the features are forwarded into two consecutive dense layers, as proposed by Huang et al. [50]. The initial dense layer applies the Rectified Linear Unit (ReLU) activation function, refining the feature set to 64 dimensions.The second dense layer, employing the softmax activation function, outputs a two-dimensional feature representing the probabilities for the FF and UF categories.

For training, we used Binary Cross Entropy (BCE) as the loss function. However, BCE can be biased toward the class with more samples in cases of imbalanced datasets, leading to a smaller loss but lower recognition accuracy for the minority class. To address this, we incorporated cost-sensitive learning by weighting the FF class (which has fewer samples) to create a weighted cross-entropy loss. The final loss function for the EBLM is given in Equation (3).

$$L_{EBLM} = \lambda L_{FF} + L_{UF}, \tag{3}$$

where LFF and LUF denote the BCE losses of the FF and UF classes, respectively. λ is the factor to balance the contribution of the losses, which is set to 4. LFF and LUF are defined in Equation (4):

$$L_{FF} = -\sum_{i=1}^{M} \sum_{j=1}^{m} y_{ij} \log (p_{ij})$$

$$L_{UF} = -\sum_{i=1}^{N} \sum_{j=1}^{m} y_{ij} \log (p_{ij}), \tag{4}$$

In this formula, *m* refers to the total number of classes. The term *yij* indicates the true label for class *j* of the *i-th* sample, which is represented using one-hot encoding. The value *pij* is the predicted probability that the *i-th* sample belongs to class *j*. Additionally, *M* and *N* represent the total number of samples for the familiar face (FF) and unfamiliar face (UF) groups, respectively.

4.1.2. CL (Confident Learning)

After performing eight-fold cross-validation on the original dataset, the EBLM module will output the probability pxj for each sample x under label j(j ∈ [0, m − 1]):

$$p_{xj} = \text{EBLM}(x), \tag{5}$$

where EBLM() depicts the EBLM module, and m represents the number of categories. An n × m probability matrix is then obtained (n is the number of samples). Note that x in Equation (5) refers to the input data, namely the red arrowhead in Figure 4.

The average probability pj (i.e., p0 and p1) for each category j is calculated as the confidence threshold:

$$C'_{y=i,\hat{y}=j} = \frac{C_{y=i,\hat{y}=j}}{\sum_{j=0}^{j=m-1} C_{y=i,\hat{y}=j}} \cdot \left|X_{y=i}\right|,$$
$$Q_{y=i,\hat{y}=j} = \frac{C'_{y=i,\hat{y}=j}}{\sum_{i=0}^{i=m-1}\sum_{j=0}^{j=m-1} C'_{y=i,\hat{y}=j}}. \tag{6}$$

Traditional confident learning (CL) methods clean data by altering samples that fall into the off-diagonal entries of the confusion matrix (such as C_confusion and C_ŷ,y* as described by Northcutt et al. [49]). However, this approach risks mistakenly pruning samples that are actually labeled correctly. To address this issue, we propose a CL method better suited for EEG-based familiarity classification.

In our approach, if a sample is predicted to belong to class *j* with the highest probability *pxj*, there are two possible cases. First, if *pxj* is greater than the confidence threshold *pj* for class *j*, it indicates that the model is confident in this prediction compared to other samples from the same class. Second, if *pxj* falls below the threshold *pj*, it suggests that the model lacks confidence in assigning the sample to class *j*, indicating a potential labeling error.

In the second scenario, if *pxj* is low, it's more likely that the sample was incorrectly labeled as class *j*. To reduce the risk of mistakenly removing correctly labeled data while still cleaning mislabeled samples, we sort the samples in *Cy=1, ŷ=0* by ascending probability and filter only the *n* × *Qy=1, ŷ=0* samples with the lowest confidence. Similarly, for samples in *Cy=0, ŷ=1*, we also select the *n* × *Qy=0, ŷ=1* with the lowest probability and update their labels to class 1.

Algorithm 1 ECL Algorithm for Familiarity Classification

Require: EEG dataset $D = \{(x_i, y_i)\}_{i=1}^{N}$, where x_i is the EEG signal and y_i is the label
Ensure: Trained EBLM model for familiarity classification
{Step 1: Construct the ERP-attention layer}
for each subject s **do**
  for each stimulus f **do**
    Crop the EEG signals x_i into epochs of 3000 ms
    Reject epochs with abnormal amplitude (outside ± 100 µV)
    Average the epochs to obtain the mean ERP values for f
  end for
end for
Calculate the attention weights $Atten(t)$ based on the ERP components through Equation (5)
{Step 2: Train the EBLM model}
Initialize the EBLM model with ERP-attention layer, Bi-LSTM layers, and dense layers
for each epoch **do**
  Feed the EEG signals x_i into the EBLM model through Equation (9)
  Compute the BCE loss L_{EBLM} considering class imbalance through Equation (7)
  Update the model parameters using Adam optimizer
end for
Perform eight-fold cross-validation on the dataset
for each sample x_i **do**
  Compute the predicted probability p_{x_i} for label j
end for
{Step 3: Perform confident learning and re-train the EBLM model}
Calculate the average probability $\overline{p_j}$ for each class j through Equation (10)
Assign pseudo-labels $\hat{y}_i$ to samples based on p_{x_i} and p_j through Equation (11)
Generate the confusion matrix $C_{y,\hat{y}}$ and normalize it to get the joint distribution matrix $Q_{y,\hat{y}}$ through Equations (12) and (13)
Prune the dataset by filtering out samples with low confidence in their pseudo-labels and re-label samples as needed
Retrain the EBLM model on the cleaned dataset
Return: The trained EBLM model for familiarity classification

5. EXPERIMENTAL RESULTS

To assess the performance of the proposed approach, experiments were carried out on both the FUFP dataset and the Wiese dataset [3]. The implementation was conducted using PyTorch on a Windows-based workstation equipped with an E5-2650 CPU and an Nvidia RTX 2080Ti GPU. For training the EBLM model, the learning rate was configured to 1 × 10^{-4}, with a maximum of 200 training epochs. The Adam optimizer was employed in conjunction with a cosine learning rate scheduler, set with a cycle period (T) of 200. The Adam optimizer was used along with a cosine learning rate scheduler, with a cycle period (T) set to 20. In accordance with the criteria outlined in Section 3, the datasets were divided into training and test sets using a 7:1 ratio. Both ablation studies and comparative experiments were performed to assess model performance.

To assess the contribution of each component in the model, it was broken down into separate modules and tested under various configurations. The outcomes of these ablation experiments are summarized in Table 1.On the FUFP dataset, using only the base EBLM model without the ERP-attention layer resulted in classification accuracy comparable to the best-performing traditional method listed in Table 5. However, once the ERP-based attention mechanism was integrated, the EBLM model achieved higher accuracy than KNN, the strongest benchmark in Table 1. This demonstrates that incorporating ERP analysis as prior knowledge enhances the model's ability to extract more meaningful features.

Next, two baseline confident learning strategies developed by Northcutt et al. [4]—Confusion Matrix (C_confusion) and Prune by Class (PBC)—were applied to the EBLM model. It's important to note that Northcutt's method, known as Prune by Noise Rate (PBNR), removes noisy samples based on a maximum margin, while the proposed method relies on sorting probabilities. After filtering the data with these approaches, a notable boost in classification accuracy was observed. Finally, applying the proposed confident learning method to clean the dataset and retraining the complete EBLM model led to an additional performance increase of 1.9%. These results indicate that the custom CL approach is particularly well-suited for handling EEG data and improving familiarity classification.

Method	**Accuracy (%)**	
	FUFP Dataset	**Wiese Dataset**
EBLM without ERP-attention layer	87	85
EBLM	89	84
EBLM + CL (baseline)	90	88
EBLM + CL (Proposed)	93	90

Table 1: Performance of Model Variants in Ablation Studies

For the Wiese dataset, the EBLM model achieved an accuracy of 89% without incorporating the ERP attention layer—an improvement of approximately 5% over the original study. In contrast, Wiese et al. employed a logistic regression-based classifier, attaining an accuracy of around 93% for FF and UF classifications. Integrating the ERP attention layer provided a slight enhancement in model performance, while the inclusion of confidence learning significantly boosted accuracy. However, its impact on the FUFP dataset was less pronounced due to the dataset's size constraints. The effectiveness of confidence learning is closely tied to dataset scale, with larger datasets yielding results more aligned with the true label distribution. Since the Wiese dataset contains fewer samples, its data-cleaning efficacy is comparatively lower than that of the FUFP dataset.

To further assess the effectiveness of our CL strategy, multiple experiments were conducted. As shown in Table 1, the proposed CL method achieved the highest accuracy by systematically filtering noise and correcting label errors within EEG datasets. The off-diagonal samples in Cy,y^C_{y,ŷ} indicate discrepancies between true and pseudo labels; however, not all these samples necessarily represent labeling errors. Directly eliminating them may inadvertently remove correctly labeled data, leading to decreased model performance. Instead, our method prioritizes noise filtering through probability sorting and refines misclassified labels rather than discarding them, ensuring maximum utilization of all samples. If an alternative approach were taken—erroneously shifting samples toward a single label—it would exacerbate class imbalance, ultimately reducing accuracy to 89%, a decline of 3% compared to conventional CL techniques. The ablation study results confirm that the proposed ECL (EBLM + CL) algorithm delivers the best performance.

This research investigates the symmetrical structure of EEG electrode placement and signal patterns, contributing to advancements in EEG-based face familiarity detection through both dataset development and methodological innovations. On the dataset front, the newly compiled FUFP dataset facilitates the implementation of supervised deep learning techniques for EEG-based face familiarity analysis. By providing a well-labeled, publicly accessible dataset with ample samples and diverse participants, it establishes a foundation for future machine learning applications in this domain.

Methodologically, the study incorporates ERP analysis into the model as attention weights, enabling the network to focus on critical signal features. The notable improvements gained through the proposed confident learning strategy highlight the importance of training models on refined, noise-reduced datasets—an aspect often overlooked in prior research. Furthermore, ERP and PSD analyses performed on the dataset provide valuable insights into the relationship between the N400 component and the recognition of familiar faces.

Additionally, it is important to clarify that the primary objective of Table 10 is not to assert the superiority of the proposed model but rather to establish a benchmark for the FUFP dataset in comparison to existing methodologies. These findings aim to support future research initiatives, fostering further exploration and refinement of EEG-based face familiarity classification techniques.

6. Conclusion

This study presents the FUFP dataset, a multi-channel, multi-label EEG dataset designed for face familiarity perception research. As the first of its kind in this field, it encompasses 6,400 samples—1,280 FF and 5,120 UF—collected from eight participants. The experimental setup used for EEG signal acquisition was extensively detailed. In addition to the dataset, we provided evaluation results obtained from five baseline classifiers, as well as ERP and PSD analyses.

Through ERP analysis, we identified four key ERP components—P1, N170, P300, and N400—that align with previous findings. Moreover, we observed a strong correlation between the N400 component and face familiarity, reinforcing earlier studies. To enhance classification performance, we introduced an algorithm that integrates ERP insights with confident learning, achieving high recognition accuracy. Moving forward, we plan to expand this algorithm to address additional EEG classification tasks.

References

[1] Young, A.W. Faces, people and the brain: The 45th Sir Frederic Bartlett Lecture. Q. J. Exp. Psychol. 2018, 71, 569–594. [CrossRef] [PubMed]

[2] Crouzet, S.M.; Kirchner, H.; Thorpe, S.J. Fast saccades toward faces: Face detection in just 100 ms. J. Vision 2010, 10, 16. [CrossRef]

[3] Morrisey, M.N.; Hofrichter, R.; Rutherford, M. Human faces capture attention and attract first saccades without longer fixation. Vis. Cogn. 2019, 27, 158–170. [CrossRef]

[4] Visconti, M.; Gobbini, M.I. Familiar face detection in 180 ms. PLoS ONE 2015, 10, e0136548.

[5] Zhang, J.; Liu, J.; Xu, Y. Neural decoding reveals impaired face configural processing in the right fusiform face area of individuals with developmental prosopagnosia. J. Neurosci. 2015, 35, 1539–1548. [CrossRef] [PubMed]

[6] DeGutis, J.; Bahierathan, K.; Barahona, K.; Lee, E.; Evans, T.; Shin, H.M.; Mishra, M.; Likitlersuang, J.; Wilmer, J. What is the prevalence of developmental prosopagnosia? An empirical assessment of different diagnostic cutoffs. Cortex 2023, 161, 51–64. [CrossRef]

[7] Zhao, Y.; Zhen, Z.; Liu, X.; Song, Y.; Liu, J. The neural network for face recognition: Insights from an fMRI study on developmental prosopagnosia. Neuroimage 2018, 169, 151–161. [CrossRef]

[8] Duchaine, B.; Yovel, G.; Nakayama, K. No global processing deficit in the navon task in 14 developmental prosopagnosics. Soc. Cogn. Affect. Neur. 2007, 2, 104–113. [CrossRef]

[9] Gu, X.; Zhang, C.; Ni, T. A hierarchical discriminative sparse representation classifier for EEG signal detection. IEEE/ACM Trans. Comput. BioL. Bioinf. 2021, 10, 1679–1687. [CrossRef]

[10] Zhang, Y.; Zhou, Z.; Pan, W.; Bai, H.; Liu, W.; Wang, L.; Lin, C. Epilepsy signal recognition using online transfer tsk fuzzy classifier underlying classification error and joint distribution consensus regularization. IEEE/ACM Trans. Comput. BioL. Bioinf. 2021, 18, 1667–1678. [CrossRef]

[11] Toyoda, A.; Ogawa, T.; Haseyama, M. MvLFDA-based video preference estimation using complementary properties of features. In

Proceedings of the IEEE International Conference on Image Processing (ICIP), Beijing, China, 17–20 September 2017; pp. 635–639.

[12] Sokolovsky, M.; Guerrero, F.; Paisarnsrisomsuk, S.; Ruiz, C.; Alvarez, S.A. Deep learning for automated feature discovery and classification of sleep stages. IEEE/ACM Trans. Comput. BioL. Bioinf. 2020, 17, 1835–1845. [CrossRef]

[13] Kanwal, S.; Uzair, M.; Ullah, H.; Khan, S.D.; Ullah, M.; Cheikh, F.A. An image based prediction model for sleep stage identification. In Proceedings of the IEEE International Conference on Image Processing (ICIP), Taipei, China, 22–25 September 2019; pp. 1366–1370

[14] Eimer, M.; Gosling, A.; Duchaine, B. Electrophysiological markers of covert face recognition in developmental prosopagnosia. Brain 2012, 135, 542–554. [CrossRef]

[15] Williams, P; White, A.; Merino, R.B.; Hardin, S.; Mizelle, J.C.; Kim, S. Facial recognition task for the classification of mild cognitive impairment with ensemble sparse classifier. In Proceedings of the Annual International Conference of the IEEE Engineering in Medicine and Biology Society (EMBC), Berlin, Germany, 23–27 July 2019; pp. 2242–2245.

[16] Tasci, I.; Baygin, M.; Barua, P.D.; Hafeez-Baig, A.; Dogan, S.; Tuncer, T.; Tan, R.S.; Acharya, U.R. Black-white hole pattern: An investigation on the automated chronic neuropathic pain detection using EEG signals. Cogn. Neurodynamics 2024, 18, 2193–2210. [CrossRef] [PubMed]

[17] Tasci, I.; Tasci, B.; Barua, P.D.; Dogan, S.; Tuncer, T.; Palmer, E.E.; Fujita, H.; Acharya, U.R. Epilepsy detection in 121 patient populations using hypercube pattern from EEG signals. Inf. Fusion 2023, 96, 252–268. [CrossRef]

[18] Lan, Z.; Liu, Y.; Sourina, O.; Wang, L.; Scherer, R.; Muller-Putz, G. SAFE: An EEG dataset for stable affective feature selection. Adv. Eng. Inf. 2020, 44, 101047. [CrossRef]

[19] Li, R.; Wang, L.; Suganthan, P.N.; Sourina, O. Sample-based data augmentation based on electroencephalogram intrinsic characteristics. IEEE J. Biomed. Health Inf. 2022, 26, 4996–5003. [CrossRef] [PubMed]